Optics Communications 501 (2021) 127359

Contents lists available at ScienceDirect

Optics Communications

journal homepage: www.elsevier.com/locate/optcom

Simultaneous turbulence mitigation and channel demultiplexing using a single multi-plane light convertor for a free-space optical link with two 100-Gbit/s OAM channels

Hao Song [a,*], Xinzhou Su [a], Haoqian Song [a], Runzhou Zhang [a], Zhe Zhao [a], Nanzhe Hu [a], Kaiheng Zou [a], Huibin Zhou [a], Kai Pang [a], Cong Liu [a], Karapet Manukyan [a], Ahmed Almaiman [a,b], Andreas F. Molisch [a], Robert W. Boyd [c,d], Shlomo Zach [e], Moshe Tur [e], Alan E. Willner [a]

[a] Department of Electrical Engineering, University of Southern California, Los Angeles, CA 90089, USA
[b] King Saud University, Riyadh, Saudi Arabia
[c] Department of Physics, University of Ottawa, Ottawa, ON, Canada
[d] Institute of Optics, University of Rochester, Rochester, New York 14627, USA
[e] School of Electrical Engineering, Tel Aviv University, Ramat Aviv 69978, Israel

ARTICLE INFO

Keywords:
Free-space optical communications
Optical vortices
Turbulence

ABSTRACT

A single multi-plane light convertor (MPLC) is applied to simultaneously mitigate turbulence-induced crosstalk and demultiplex two orbital angular momentum (OAM) multiplexed channels for a free-space optical link. Comprised of six programmable phase planes, the MPLC is placed at the receiver side for turbulence mitigation and channel demultiplexing. Propagating through the cascaded phase planes, two coaxial turbulence-distorted OAM beams each carrying one data channel are shaped and sorted into two differently positioned Gaussian beams with low inter-channel crosstalk. As an experimental demonstration, one MPLC adaptively mitigates the turbulence-induced crosstalk by up to 26 dB for two OAM-multiplexed channels (ℓ = {−1, +2}). Two 100-Gbit/s quadrature-phase-shift-keying (QPSK) channels are recovered with an up-to-1.5-dB optical signal-to-noise ratio (OSNR) penalty under one turbulence realization.

1. Introduction

Multi-plane light convertor (MPLC) is a technique for spatial transformation of optical fields by multiple cascaded phase planes separated in free space [1–7]. It has been theoretically shown that MPLC could perform a unitary transformation given adequate number of discrete phase planes [8]. One type of such unitary transformation is "mode sorting" which converts coaxial orthogonal spatial modes from a modal basis set to Gaussian modes with different transverse spatial locations [8,9]. Such "mode sorting" function has been used to achieve channel demultiplexing in a mode-division-multiplexing (MDM) free-space optical (FSO) communication link [10].

Separately, the MPLC-related multi-mode-receiver approach has been applied for turbulence mitigation in a single-channel FSO link [11]. In an FSO communication link, the atmospheric turbulence could distort the wavefront or cause beam wandering [12,13]. This could lead to power coupling from a fundamental Gaussian mode to higher-order modes and thus induce power fluctuation at the receiver [14,15]. With the help of MPLC-based "mode sorting" function, the signal power in higher-order modes is captured, sorted into separate receivers, combined digitally and thus the turbulence-induced power fluctuation of a single channel is reduced [11].

Moreover, in an MDM FSO link under turbulence effects, one may want to both mitigate turbulence-induced inter-channel crosstalk and demultiplex channels each carried by an orthogonal spatial mode. It would be interesting to extend the MPLC-based spatial transformation to correct the turbulence-distorted wavefront and thus reduce inter-channel crosstalk in an MDM FSO link. Moreover, using the same MPLC, wavefront correction function and "mode sorting" function could be combined and applied [16]. In the previous experimental work [16], the MPLC was applied to achieve the turbulence mitigation function and the channel demultiplexing function for a fixed mode set (i.e., ℓ = {0, +1}) and the turbulence mitigation performance with a different number of mitigation planes was not discussed.

In this paper, we experimentally utilize a single MPLC to simultaneously mitigate turbulence-induced crosstalk and demultiplex channels for an FSO link with two orbital angular momentum (OAM) multiplexed channels each carrying a 100 Gbit/s quadrature-phase-shift-keying (QPSK) signal. The turbulence-distorted wavefronts of the

* Corresponding author.
E-mail address: songhao@usc.edu (H. Song).

https://doi.org/10.1016/j.optcom.2021.127359
Received 28 May 2021; Received in revised form 26 July 2021; Accepted 8 August 2021
Available online 10 August 2021

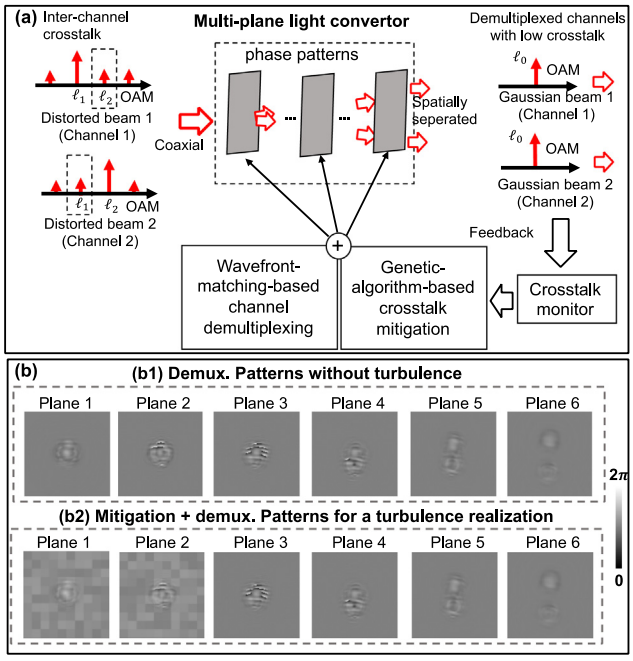

Fig. 1. (a) Concept of utilizing one MPLC to simultaneously mitigate turbulence-induced crosstalk and demultiplex OAM channels. The turbulence distorts the coaxial OAM beams and introduces power coupling among multiple neighboring modes before coupling into the MPLC. The phase patterns of MPLC are initialized for channel demultiplexing without considering turbulence distortion. With the feedback of the monitored inter-channel crosstalk, the genetic algorithm is applied to adaptively update the phase patterns of MPLC. Subsequently, each distorted beam propagates through the cascaded phase patterns and gets converted to the corresponding Gaussian beam with relatively low inter-channel crosstalk. (b) Examples of the (b1) phase patterns for channel demultiplexing and (b2) superimposed mitigation and demultiplexing patterns for a turbulence realization.

data-carrying beams are shaped by the six cascaded phase plates of MPLC. The experimental results show that (i) the MPLC can be reconfigured to mitigate turbulence-induced crosstalk for OAM-carried channels with different mode sets ($\ell = \{-1, +2\}$ or $\ell = \{-1, +1\}$), (ii) the crosstalk is mitigated by up to 26 dB for OAM-multiplexed channels (i.e., $\ell = \{-1, +2\}$) under 10 turbulence realizations ($D/r_0 < 1.7$); and (iii) the bit error rate (BER) at the 3.8×10^{-3} forward error correction (FEC) threshold level is achieved with an optical signal-to-noise ratio (OSNR) penalty of up to 1.5 dB for two OAM channels (i.e., $\ell = \{-1, +2\}$) under one turbulence realization.

2. Concept of MPLC

Fig. 1 (a) shows the concept of utilizing one MPLC to simultaneously mitigate turbulence-induced crosstalk and demultiplex OAM channels. Two OAM beams each carrying an independent data channel are transmitted coaxially. The wavefronts of the coaxial OAM beams are distorted by the atmospheric turbulence, which introduces the power coupling among multiple neighboring modes and leads to inter-channel crosstalk. Subsequently, the spatial profiles of the distorted coaxial OAM beams are shaped while propagating through the cascaded phase planes in the MPLC. The phase planes are adaptively generated to simultaneously mitigate turbulence-induced crosstalk and demultiplex OAM channels. After propagating through the MPLC, the two distorted OAM beams are converted to two differently positioned Gaussian beams with low inter-channel crosstalk.

The phase patterns of the MPLC are generated by utilizing the wavefront matching method [6] and the genetic algorithm (GA) [17,18]. Fig. 1(b1) shows the phase patterns for channel demultiplexing. Fig. 1(b2) shows the phase patterns which are superimposed of demultiplexing patterns and mitigation patterns for one turbulence realization. A wavefront matching method is utilized to pre-calculate the demultiplexing phase patterns [6]. The wavefront matching method works as an optimization process to point-to-point match the phase of each pair of input (*i.e.*, the OAM beam with a specific mode order) and output (*i.e.*, the Gaussian beam with a specific position) with multiple phase patterns. For demultiplexing two modes (k = 2) using MPLC, five phase plates (2k+1 = 5) are typically needed to achieve a relatively high mode purity [8]. As proof of concept, we utilize six phase plates to achieve two-mode demultiplexing. By increasing the number of phase plates, the MPLC could potentially achieve a higher conversion efficiency [6]. The pattern-to-pattern spacing is chosen as 31.5 mm. We choose such a pattern-to-pattern spacing by considering several experimental limitations, including the width of the mirror and the incident angle of the light beam. On one hand, if a larger pattern-to-pattern spacing is chosen, there could be larger beam divergence and thus the output beam might be truncated by the mirror. On the other hand, for a smaller pattern-to-pattern spacing, a larger incident angle might be required to keep the same number of reflections which might reduce the phase modulation efficiency of the SLM [19].

Subsequently, the GA is applied iteratively to search for the optimized mitigation patterns in order to minimize the highest crosstalk among the OAM channels. The GA stops when reaching a crosstalk threshold of <−18 dB or 1000 iterations. It should be noted that all the mitigation patterns and demultiplexing patterns are allocated in the same SLM. However, the demultiplexing patterns and mitigation patterns consist of a different number of elements (i.e., the minimum components of each phase pattern). The pixel size of the SLM is 9.2 μm. To fully utilize the spatial resolution of the SLM, each demultiplexing pattern has 300 × 300 elements. Each element occupies one pixel of the SLM (9.2 μm for each element). However, the optimization time of the GA used to optimize the mitigation patterns partially depends on the number of elements [20]. To optimize the mitigation patterns at a faster speed for different turbulence realizations, each mitigation pattern has a smaller number of elements compared to the demultiplexing pattern. In this case, each mitigation pattern has 10 × 10 elements and each element occupies 30 × 30 pixels of the SLM (276 μm for each element). In general, an increasing number of pixels or an increasing number of mitigation patterns could potentially provide more degrees of freedom while it might also require a more efficient optimization algorithm [20].

As proof of concept, we set the locations of the two mitigation planes at plane 1 and plane 2. It should be noted that the performance of turbulence mitigation might be different when there is a different arrangement of the mitigation planes. For example, when two mitigation planes are set at plane 5 and plane 6 or even separately at plane 4 and plane 6, the distorted coaxial beams are first partially separated and then spatially modulated by the mitigation planes. Compared to the arrangement used in our experiment, larger mitigation patterns might be needed due to the beam separation. This could potentially induce different crosstalk performance and require a different number of iterations [21].

3. Experimental setup

The experimental setup is shown in Fig. 2. At the transmitter side, the 100-Gbit/s QPSK signal with the center wavelength of 1550 nm is equally split by a 50/50 coupler and the two signal copies are decorrelated by passing through fibers with different path lengths. The two fiber branches are fed into two input ports of a channel multiplexer, whose free-space output comprises two multiplexed OAM beams. The polarization controllers are used to maximize the polarization-sensitive modulation efficiency of the SLM-based MPLC. It is also possible to use a polarization-insensitive configuration [22]. A channel multiplexer is used to generate different coaxial OAM beams by feeding different fiber ports. The channel multiplexer itself is an MPLC-based device

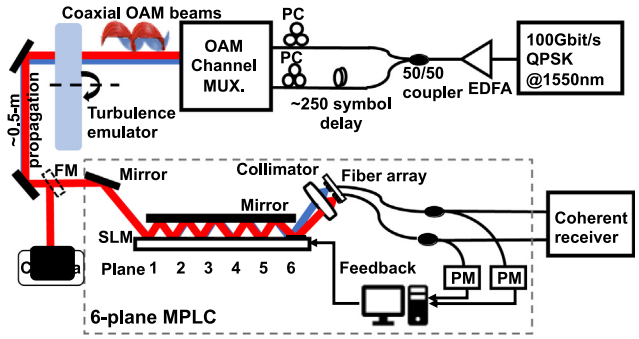

Fig. 2. Experimental setup of using MPLC for turbulence-induced crosstalk mitigation and channel demultiplexing in an OAM-multiplexed link. QPSK: quadrature phase-shift keying. EDFA: erbium-doped fiber amplifier. PC: polarization controller. Mux: multiplexer. SLM: spatial light modulator. PM: power meter. FM: flip mirror.

where the beams are reflected multiple times at different locations on a fixed reflective phase plate [8,10]. Subsequently, the OAM beams with a beam size D of <1.7 mm is normally incident on the emulated turbulence plate with an effective Fried parameter (coherence length scale of turbulence) of r_0 = 1 mm [23–25]. The turbulence plate has a pseudorandom phase distribution that obeys Kolmogorov spectrum statistics. After ~0.5-m free-space propagation, the distorted beams are projected onto the first plane (with the equivalent aperture size of ~2.7 mm) of the SLM (Meadowlark Optics). Serving as an MPLC, the SLM is positioned parallel to a silver mirror with a spacing of ~15.7 mm. The beams are bounced between the mirror and the SLM to go through six different phase planes with an adjacent free-space propagation distance of 31.5 mm. After passing through the six-plane MPLC, the two beams are separated spatially and coupled into different ports of the fiber array with a spacing of 127 μm using a single collimator (NA = 0.35). After the power collection of both ports, a feedback loop is designed to monitor the crosstalk between the two channels. Given the measured crosstalk, a GA is applied in order to update the patterns to mitigate the turbulence effect. After the MPLC patterns are optimized, the signals carried by the two transmitted OAM beams are received for coherent signal detection with low inter-channel crosstalk.

4. Experimental results

In the experiment, we first characterize the channel demultiplexing using MPLC. At the transmitter side, a single OAM beam is generated and transmitted one at a time. At the receiver side, the demultiplexing patterns are generated for two different cases, *i.e.*, OAM-multiplexed channels ℓ = {−1, +1} and {−1, +2}. Fig. 3(a1, b1) shows that the inter-channel crosstalk is <−22 dB and <−19 dB for the OAM-multiplexed channels of ℓ = {−1, +1} and {−1, +2}, respectively. To investigate the turbulence mitigation of the MPLC, we put a rotatable turbulence emulator in the free-space optical path. After passing through the turbulence emulator, the distorted coaxial OAM beams are demultiplexed by the MPLC. Fig. 3(a2, b2) shows that, compared with the cases without turbulence, the crosstalk degradation in the cases with turbulence and without crosstalk mitigation is >13.1 dB and >9.2 dB for the transmitted OAM channels ℓ = {−1, +1} and {−1, +2}, respectively. After applying crosstalk mitigation, the crosstalk is mitigated by >11.4 dB and >7.2 dB for the transmitted OAM channels ℓ = {−1, +1} and {−1, +2}, respectively, as shown in Fig. 3(a3, b3). The turbulence-induced power loss is also reduced simultaneously. It should be noted that, for both ℓ = {−1, +1} and {−1, +2}, the insertion loss of the MPLC is <−19 dB, >−23 dB and <−20 dB without turbulence, without and with turbulence mitigation, respectively. The insertion loss of the designed mode might be limited by the reflection coefficient and

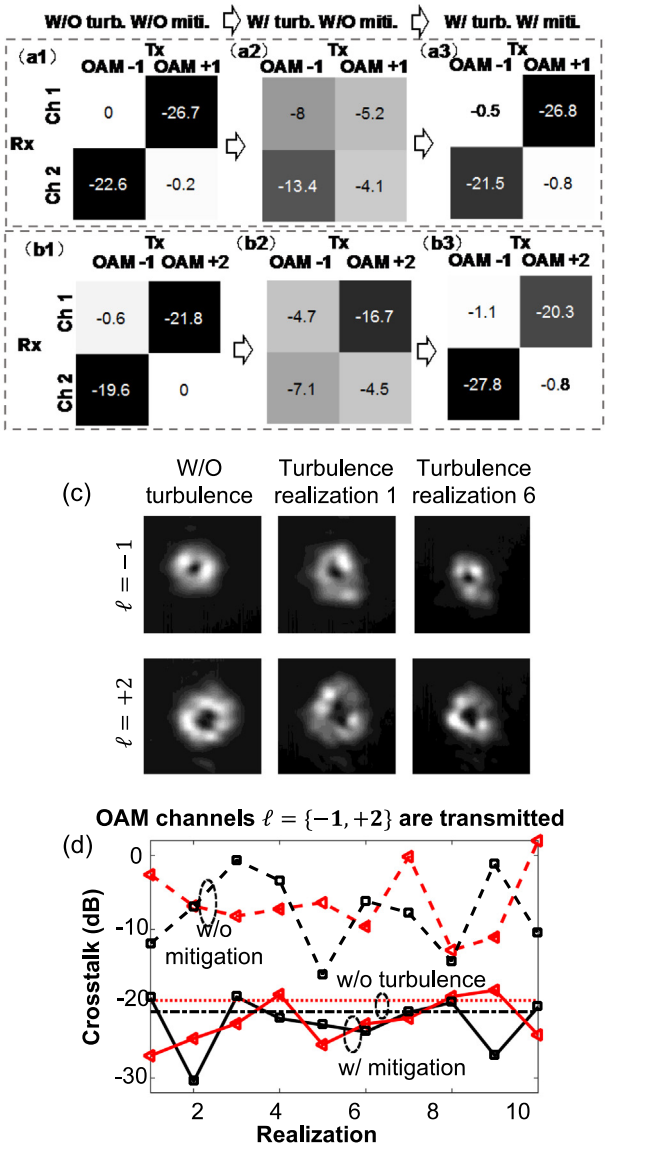

Fig. 3. Measured transmission matrix of OAM-multiplexed channels. (a1–a3) ℓ = −1 and +1, (b1–b3) ℓ = −1 and ℓ = +2 for channel demultiplexing without turbulence, without and with crosstalk mitigation (miti.) under the turbulence (turb.). (c) Beam profiles of ℓ = −1 and +2 without turbulence and with turbulence under different realizations. (d) Measured crosstalk without (dashed line) and with (solid line) mitigation for the channels carried by ℓ = −1 (black line) and ℓ = +2 (red line) under 10 turbulence realizations.

the grating efficiency of the SLM. With a lossless SLM without blaze gratings [3,6], the insertion loss of the MPLC could be ~−2 dB with turbulence mitigation. It should be noted that the insertion loss of the MPLC-based device might be related to the number of phase plates [6]. In general, the insertion loss related to the reflection coefficient and the grating efficiency could be decreased by utilizing a smaller number of phase plates. However, reducing the number of phase plates tends to achieve less adiabatic spatial phase modulation and could potentially decrease the conversion efficiency [6].

Furthermore, different realizations of the turbulence are emulated by rotating the turbulence emulator. For each measurement under different realizations, the turbulence phase plate is fixed and the beams are transmitted through a different part of the turbulence emulator [24,25]. As a proof of concept, the OAM-multiplexed channels of ℓ = −1 and +2 are transmitted. Fig. 3(c) shows the beam profiles

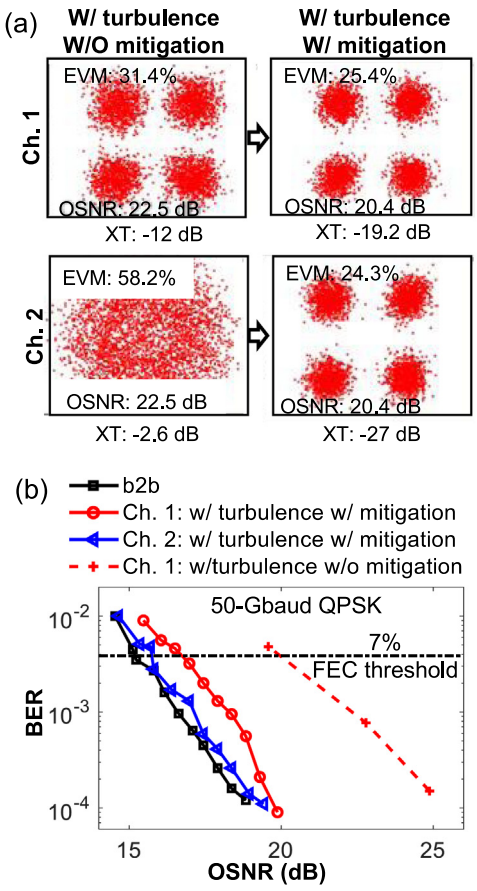

Fig. 4. Measured bit error rates (BERs) performance for multiplexed data channel 1 ($\ell = -1$) and 2 ($\ell = +2$) with and without turbulence mitigation (a) Constellation diagrams for QPSK signal; (b) BER vs OSNR. Ch: channel. XT: crosstalk. FEC: forward error correction. EVM: error vector magnitude.

of the OAM $\ell = -1$ and $+2$ are distorted differently under different turbulence realizations which could lead to varying inter-channel crosstalk. Such beam profiles are captured at the input side of the MPLC. It should be noted that, the beam profiles are not perfect without turbulence [10]. The intermodal crosstalk between $\ell = -1$ and $\ell = +2$ without turbulence is <−25 dB. This might be due to imperfect performance of the channel multiplexer. Fig. 3(d) shows that under 10 different turbulence realizations before applying turbulence mitigation, the crosstalk of channel 1 ($\ell = -1$) and channel 2 ($\ell = +2$) varies from −0.8 dB to −16.2 dB and from −12.8 dB to 2.0 dB, respectively. After applying turbulence mitigation, the crosstalk under −18 dB and a crosstalk reduction of up to 26 dB are achieved for both channels. Under some specific turbulence realizations, the inter-channel crosstalk after turbulence mitigation is lower than that without turbulence. This might be due to that the MPLC mitigates the crosstalk induced by not only the turbulence but also residual misalignment [18,26].

Under turbulence realization 1, the BER performance is measured by transmitting the OAM-multiplexed ($\ell = \{-1, +2\}$) channels simultaneously. As shown in Fig. 4(a), the measured crosstalk for channel 1 ($\ell = -1$) and channel 2 ($\ell = +2$) mode are decreased from −12 dB and −2.6 dB to −19.2 dB and −27 dB and the error vector magnitude (EVM) is improved from 31% and 58% to 25% and 24%, respectively, by applying the turbulence mitigation. Fig. 4(b) shows that without turbulence mitigation, there is ~4.8 dB OSNR penalty for channel 1 to achieve BER of 3.8×10^{-3}(*i.e.*, 7% FEC threshold) compared with that of back-to-back case. For channel 2 ($\ell = +2$) without turbulence mitigation, the coherent detection algorithm does not readily recover the I-Q information. After applying turbulence mitigation, there is

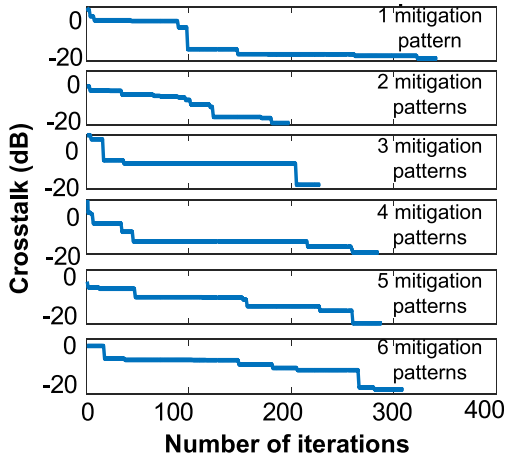

Fig. 5. Measured crosstalk with different number of mitigation patterns applied under one turbulence realization in experiment for OAM-multiplexed channels $\ell = \{-1,+2\}$.

~0.5 and ~1.5 dB OSNR penalty to achieve the 7% FEC threshold compared with that of the back-to-back case for channel 1 and channel 2, respectively. The difference in the OSNR penalty might be due to the different crosstalk of different channels.

As the generation of demultiplexing patterns and mitigation patterns is relatively independent, the number of mitigation patterns is not necessarily the same as that of demultiplexing patterns. To explore the effect of the number of mitigation patterns, the number of mitigation patterns is varied from 1 to 6. Fig. 5 shows that the cases with a different number of mitigation patterns achieve similar crosstalk mitigation performance while the two-plane case takes the lowest number of iterations. This might be due to that, with the increasing number of mitigation patterns, the increased degree of freedom tends to increase the optimization speed while also increase the search space that might limit the optimization speed [21,27].

5. Simulation results

In addition, we further explore the turbulence mitigation using different number of mitigation planes under 200 turbulence realizations in simulation. Fig. 6 (a, b) show that (i) the crosstalk could be achieved below the crosstalk threshold of −18 dB and sometimes <−25 dB, and (ii) the number of iterations could range from ~50 to ~700. The average number of iterations could partially depend on the number of mitigation planes. The simulation result shows that, when the number of mitigation planes increases from 1 to 6, the average number of iterations taken to reach the crosstalk level under −18 dB is ~250, ~160, ~170, ~180, ~200 and ~200, respectively. The case with two mitigation planes could achieve the crosstalk below −18 dB with the smallest average number of iterations. This might be due to that, when the number of mitigation patterns increases, the increased degrees of freedom tend to increase the optimization speed but could also increase the search space that might limit the optimization speed [21,27]. Moreover, we use two turbulence simulation approaches: (a) single phase plate in order to replicate our experimental demonstration, (b) two phase plates in order to have better accuracy for thicker turbulent layers [25,28]. For the case with two turbulence plates, we use the same Fried parameter $r_0 = 1$ mm as the case of a single turbulence plate (red-dashed line) [28]. In such a scenario, the two cases with different turbulence plates show a similar trend of crosstalk performance and average iteration number. It should be noted that the number of iterations might be related to various parameters that include but are not limited to the crosstalk threshold and the optimization algorithm [20].

To investigate the scalability of the MPLC for turbulence mitigation, we apply the same method to the OAM mode sets with a different

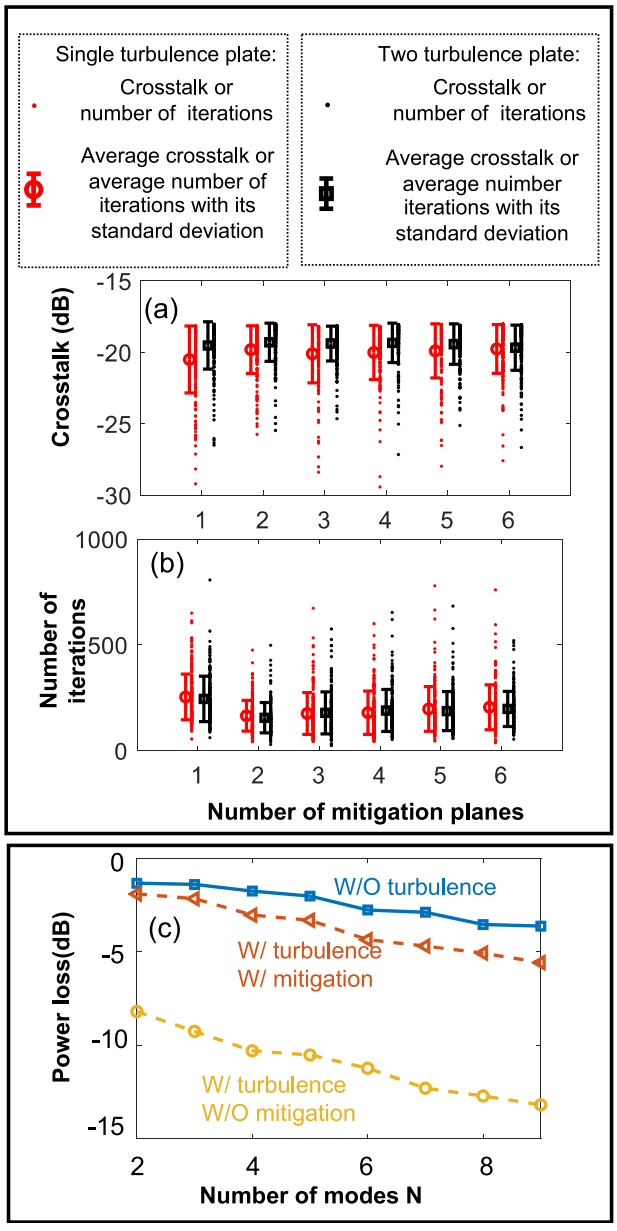

Fig. 6. Simulated (a) crosstalk and (b) number of iterations under 200 turbulence realizations for OAM-multiplexed channel $\ell = \{-1, +2\}$. Each red/black dot represents the simulated crosstalk and the simulated number of iterations under one turbulence realization emulated by a single turbulence plate/two turbulence plates. The circles/squares represent the simulated average crosstalk and the simulated average number of iterations under 200 turbulence realizations emulated by a single turbulence plate/two turbulence plates. The bars show the corresponding standard deviation values. (c) Simulated average insertion loss of the MPLC without turbulence, without and with mitigation under 100 turbulence realizations.

number of modes in simulation under 100 turbulence realizations. It should be noted that the power loss induced by MPLC might depend on (i) the spatial modulation efficiency related to the reflection coefficient and the grating efficiency of the SLM, (ii) the channel demultiplexing, and (iii) the turbulence mitigation [6,8,29]. In our simulation, to separate the influence of the SLM's modulation efficiency from channel demultiplexing and turbulence mitigation, each phase plate is assumed to be lossless. Therefore, the modulation efficiency of the SLM is not included in the simulated power loss. As a proof of concept, the first N (N < 10) OAM modes are selected from the sequence of OAM ℓ = (0, +1, −1, +2, −2, +3, −3, +4, −4) and two mitigation patterns are adaptively applied in the MPLC. Fig. 6(c) shows that the turbulence-induced power losses of 6–9 dB are induced on average under 100 turbulence realizations without applying turbulence mitigation. After the corresponding turbulence mitigation is applied, the average insertion loss of MPLC is reduced. This could be due to that the mitigation patterns not only reduce the inter-channel crosstalk but also mitigate the power coupling to the other higher-order modes [29].

6. Discussion

To mitigate the turbulence effects on an MDM FSO link, there have been various approaches including (i) adaptive optics which applies an inverse phase function of turbulence to mitigate inter-modal crosstalk [29–33] and (ii) electronic digital signal processing based on multiple-input-multiple-output (MIMO) equalization [34,35]. We note that there are some challenges to minimize the system complexity for the proposed MPLC-based approach. It would be valuable to develop a more efficient method for the MPLC system.

In our demonstration, we need to periodically update the phase patterns and measure the mode transmission matrix of the two channels. During the measurement of transmission matrix, we: (a) interrupt the transmitted data flow of the two data channels, (b) sequentially transmit only one OAM beam at a time, and (c) for each OAM beam, we measure the power in each part of the full mode transmission matrix. Subsequently, the two data channels can then be transmitted simultaneously. Importantly, this periodic interruption of data transmission can potentially be avoided by utilizing probe beams that: (i) experience similar turbulence effect, and (ii) could be separated from the transmitted data channels with little power coupling. Possible methods include (a) utilizing coaxial OAM probe beams at different wavelengths [29] or (b) transmitting coaxial backward-propagating probe beams from the receiver to the transmitter and measuring the crosstalk at the transmitter [36].

Additionally, we note that real-time turbulence mitigation approaches in an FSO link should be operated as fast as the dynamic decoherence effects of the turbulence, perhaps at a rate of ~kHz [23,25]. In our demonstration, it takes ~5 s for each iteration and ~200 iterations to mitigate the turbulence-induced crosstalk. This would be too slow in a practical link, but the speed could be significantly increased by various methods. In order to decrease the operation time of each iteration and increase the speed of turbulence mitigation, one might consider: (i) applying a more efficient optimization algorithm to reduce the number of iterations, such as a parallel wavefront optimization method [20] and (ii) utilizing a high-speed wavefront modulator [37].

Declaration of competing interest

The authors declare that they have no known competing financial interests or personal relationships that could have appeared to influence the work reported in this paper.

Acknowledgments

We acknowledge the generous support of Vannevar Bush Faculty Fellowship program from ASD (R&E) and Office of Naval Research (ONR) through grant N00014-16-1-2813; Defense Advanced Research Projects Agency (DARPA) W911NF-18-0369; Defense Security Cooperation Agency (DSCA-4440646262); National Science Foundation (NSF) ECCS-1509965; Office of Naval Research through a MURI grant N00014-20-1-2558.

References

[1] G. Labroille, B. Denolle, P. Jian, P. Genevaux, N. Treps, J.-F. Morizur, Efficient and mode selective spatial mode multiplexer based on multi-plane light conversion, Opt. Express 22 (2014) 15599.

[2] Y. Zhang, N.K. Fontaine, H. Chen, R. Ryf, D. Neilson, J. Carpenter, G. Li, An ultra-broadband polarization-insensitive optical hybrid using multiplane light conversion, J. Lightwave Technol. (2020) 6286.

[3] Z. Lin, Y. Wen, Y. Chen, S. Yu, Transmissive multi-plane light conversion for demultiplexing orbital angular momentum modes, in: 2020 Conference on Lasers and Electro-Optics, 2020, p. SF1J.5.

[4] N.K. Fontaine, R. Ryf, H. Chen, D.T. Neilson, K. Kim, J. Carpenter, Scalable mode sorter supporting 210 Hermite-Gaussian modes, in: 2018 Optical Fiber Communications Conference and Exposition, 2018, p. Th4B.4.

[5] M. Hiekkamäki, S. Prabhakar, R. Fickler, Near-perfect measuring of full-field transverse-spatial modes of light, Opt. Express 27 (2019) 31456–31464.

[6] N.K. Fontaine, R. Ryf, H. Chen, D.T. Neilson, K. Kim, J. Carpenter, Laguerre-Gaussian mode sorter, Nature Commun. 10 (2019) 1865.

[7] H. Wen, Y. Zhang, R. Sampson, N.K. Fontaine, N. Wang, S. Fan, G. Li, Scalable non-mode selective Hermite-Gaussian mode multiplexer based on multi-plane light conversion, Photon. Res. PRJ 9 (2021) 88–97.

[8] J.-F. Morizur, L. Nicholls, P. Jian, S. Armstrong, N. Treps, B. Hage, M. Hsu, W. Bowen, J. Janousek, H.-A. Bachor, Programmable unitary spatial mode manipulation, J. Opt. Soc. Amer. A 27 (2010) 2524.

[9] G.C.G. Berkhout, M.P.J. Lavery, J. Courtial, M.W. Beijersbergen, M.J. Padgett, Efficient sorting of orbital angular momentum states of light, Phys. Rev. Lett. 105 (2010) 153601.

[10] L. Li, R. Zhang, Z. Zhao, G. Xie, P. Liao, K. Pang, H. Song, C. Liu, Y. Ren, G. Labroille, P. Jian, D. Starodubov, B. Lynn, R. Bock, M. Tur, A.E. Willner, High-capacity free-space optical communications between a ground transmitter and a ground receiver via a UAV using multiplexing of multiple orbital-angular-momentum beams, Sci. Rep. 7 (2017) 17427.

[11] N.K. Fontaine, R. Ryf, Y. Zhang, J.C. Alvarado-Zacarias, H. Huang, H. Chen, R. Amezcua-Correa, G. Li, M. Capuzzo, R. Kopf, A. Tate, H. Safar, C. Bolle, D.T. Neilson, E. Burrows, K. Kim, M. Bigot-Astruc, F. Achten, P. Sillard, A. Amezcua-Correa, J. Carpenter, Digital turbulence compensation of free space optical link with multimode optical amplifier, in: 2019 European Conference on Optical Communication, 2019.

[12] D. Kedar, S. Arnon, Urban optical wireless communication networks: the main challenges and possible solutions, IEEE Commun. Mag. 42 (2004) S2.

[13] M.A. Khalighi, M. Uysal, Survey on free space optical communication: A communication theory perspective, IEEE Commun. Surv. Tutor. 16 (2014) 2231.

[14] R.J. Noll, Zernike polynomials and atmospheric turbulence, J. Opt. Soc. Amer. 66 (1976) 207.

[15] Y. Dikmelik, F.M. Davidson, Fiber-coupling efficiency for free-space optical communication through atmospheric turbulence, Appl. Opt. 44 (2005) 4946.

[16] H. Song, X. Su, H. Song, R. Zhang, Z. Zhao, C. Liu, K. Pang, N. Hu, A. Almaiman, A. Almaiman, S. Zach, N. Cohen, A. Molisch, R. Boyd, R. Boyd, M. Tur, A.E. Willner, Simultaneous turbulence mitigation and mode demultiplexing using one MPLC in a two-mode 200-Gbit/s free-space OAM-multiplexed Link, in: 2020 Optical Fiber Communications Conference, Optical Society of America, 2020, p. W1G.3.

[17] R. Fickler, M. Ginoya, R.W. Boyd, Custom-tailored spatial mode sorting by controlled random scattering, Phys. Rev. B 95 (2017) 161108.

[18] R. Zhang, H. Song, Z. Zhao, H. Song, J. Du, C. Liu, K. Pang, L. Li, H. Zhou, A.N. Willner, A. Almaiman, Y. Zhou, R.W. Boyd, B. Lynn, R. Bock, M. Tur, A.E. Willner, Simultaneous turbulence mitigation and channel demultiplexing for two 100 Gbit/s orbital-angular-momentum multiplexed beams by adaptive wavefront shaping and diffusing, Opt. Lett. 45 (2020) 702.

[19] A. Lizana, N. Martín, M. Estapé, E. Fernández, I. Moreno, A. Márquez, C. Iemmi, J. Campos, M.J. Yzuel, Influence of the incident angle in the performance of liquid crystal on silicon displays, Opt. Express 17 (2009) 8491.

[20] M. Cui, Parallel wavefront optimization method for focusing light through random scattering media, Opt. Lett. 36 (2011) 870.

[21] P. Rajaeipour, K. Banerjee, A. Dorn, H. Zappe, Ç. Ataman, Cascading optofluidic phase modulators for performance enhancement in refractive adaptive optics, Adv. Photonics 2 (2020) 066005.

[22] J. Liu, J. Wang, Demonstration of polarization-insensitive spatial light modulation using a single polarization-sensitive spatial light modulator, Sci. Rep. 5 (2015) 9959.

[23] C. Paterson, Atmospheric turbulence and orbital angular momentum of single photons for optical communication, Phys. Rev. Lett. 94 (2005) 153901.

[24] Y. Ren, H. Huang, G. Xie, N. Ahmed, Y. Yan, B.I. Erkmen, N. Chandrasekaran, M.P.J. Lavery, N.K. Steinhoff, M. Tur, S. Dolinar, M. Neifeld, M.J. Padgett, R.W. Boyd, J.H. Shapiro, A.E. Willner, Atmospheric turbulence effects on the performance of a free space optical link employing orbital angular momentum multiplexing, Opt. Lett. 38 (2013) 4062.

[25] L.C. Andrews, R.L. Phillips, Laser Beam Propagation Through Random Media, SPIE, 2005.

[26] G. Xie, L. Li, Y. Ren, H. Huang, Y. Yan, N. Ahmed, Z. Zhao, M.P.J. Lavery, N. Ashrafi, S. Ashrafi, R. Bock, M. Tur, A.F. Molisch, A.E. Willner, Performance metrics and design considerations for a free-space optical orbital-angular-momentum-multiplexed communication link, Optica 2 (2015) 357.

[27] M. Gen, L. Lin, Genetic Algorithms, American Cancer Society, 2008.

[28] B. Rodenburg, M. Mirhosseini, M. Malik, O.S. Magaña Loaiza, M. Yanakas, L. Maher, N.K. Steinhoff, G.A. Tyler, R.W. Boyd, Simulating thick atmospheric turbulence in the lab with application to orbital angular momentum communication, New J. Phys. 16 (2014) 033020.

[29] Y. Ren, G. Xie, H. Huang, L. Li, N. Ahmed, Y. Yan, M.P.J. Lavery, R. Bock, M. Tur, M.A. Neifeld, R.W. Boyd, J.H. Shapiro, A.E. Willner, Turbulence compensation of an orbital angular momentum and polarization-multiplexed link using a data-carrying beacon on a separate wavelength, Opt. Lett. 40 (2015) 2249.

[30] Y. Ren, G. Xie, H. Huang, N. Ahmed, Y. Yan, L. Li, C. Bao, M.P.J. Lavery, M. Tur, M.A. Neifeld, R.W. Boyd, J.H. Shapiro, A.E. Willner, Adaptive-optics-based simultaneous pre- and post-turbulence compensation of multiple orbital-angular-momentum beams in a bidirectional free-space optical link, Optica 1 (2014) 376.

[31] S. Li, J. Wang, Compensation of a distorted N-fold orbital angular momentum multicasting link using adaptive optics, Opt. Lett. 41 (2016) 1482.

[32] M. Li, M. Cvijetic, Y. Takashima, Z. Yu, Evaluation of channel capacities of OAM-based FSO link with real-time wavefront correction by adaptive optics, Opt. Express 22 (2014) 31337–31346.

[33] M. Li, Y. Takashima, X. Sun, Z. Yu, M. Cvijetic, Enhancement of channel capacity of OAM-based FSO link by correction of distorted wave-front under strong turbulence, in: Frontiers in Optics 2014, OSA, 2014, p. FTh3B.6.

[34] H. Huang, Y. Cao, G. Xie, Y. Ren, Y. Yan, C. Bao, N. Ahmed, M.A. Neifeld, S.J. Dolinar, A.E. Willner, Crosstalk mitigation in a free-space orbital angular momentum multiplexed communication link using 4x4 MIMO equalization, Opt. Lett. 39 (2014) 4360.

[35] Y. Zhang, P. Wang, L. Guo, W. Wang, H. Tian, Performance analysis of an OAM multiplexing-based MIMO FSO system over atmospheric turbulence using space–time coding with channel estimation, Opt. Express 25 (2017) 19995.

[36] S. Bae, Y. Jung, B.G. Kim, Y.C. Chung, Compensation of mode crosstalk in MDM system using digital optical phase conjugation, IEEE Photon. Technol. Lett. 31 (2019) 739.

[37] O. Tzang, E. Niv, S. Singh, S. Labouesse, G. Myatt, R. Piestun, Wavefront shaping in complex media with a 350 kHz modulator via a 1D-to-2D transform, Nature Photon. 13 (2019) 788.